



# Quantum Sensing $1/f$ Noise via Pulsed Control of a Two-Qubit Gate<sup>†</sup>

Antonio D'Arrigo<sup>1</sup>, Giuseppe Falci<sup>1,2,3</sup>  and Elisabetta Paladino<sup>1,2,3,\*</sup> 

<sup>1</sup> Dipartimento di Fisica e Astronomia, Università di Catania, Via S. Sofia 64, 95123 Catania, Italy

<sup>2</sup> CNR-IMM, Catania Università, Via S. Sofia 64, 95123 Catania, Italy

<sup>3</sup> Istituto Nazionale di Fisica Nucleare, Sez. di Catania, Via Santa Sofia 64, 95123 Catania, Italy

\* Correspondence: epaladino@dmfci.unict.it; Tel.: +39-095-378-5501

<sup>†</sup> Presented at the 11th Italian Quantum Information Science conference (IQIS2018), Catania, Italy, 17–20 September 2018.

Published: 25 July 2019



**Abstract:** Dynamical decoupling sequences are a convenient tool to reduce decoherence due to intrinsic fluctuations with  $1/f$  power spectrum hindering quantum circuits. We study the possibility to achieve an efficient universal two-qubit gate in the presence of  $1/f$  noise by periodic and Carr-Purcell dynamical decoupling. The high degree of selectivity achieved by these protocols also provides a valuable tool to infer noise characteristics, as the high-frequency cut off and the noise variance. Different scalings of the gate error with noise variance signal the contribution of different noise statistical properties to the gate error.

**Keywords:**  $1/f$  noise; quantum sensing; dynamical decoupling; quantum gates

## 1. Introduction

In the race towards quantum technologies, superconducting nanocircuits are at the forefront of the next generation of quantum processing units for hybrid quantum processors exploiting the best computational characteristics of the currently available quantum devices (solid-state quantum hardware, quantum optics setups etc.) [1,2]. Since the early experiments, superconducting quantum circuits revealed their potentialities of tunability and large-scale scalability making them potential candidates for the implementation of quantum gates [3]. Their main limitations were low gate fidelities due to material-inherent noise sources characterized by  $1/f$  power spectrum at low frequencies [4]. Clear signatures of bistable fluctuations induced by the same intrinsic noise sources were also reported [4,5]. These limitations have been progressively reduced via device design, improved materials and control protocols [6–8]. Presently, quality factors of single-qubit gates satisfy the criteria required for quantum error correcting codes [9] whereas further improvement is needed for two-qubit gates [10] and small quantum-nodes of complex networks. Advanced quantum protocols based on pulsed control represent a viable strategy towards this goal [11–25]. In superconducting qubits dephasing due to charge- and magnetic flux-noise has been reduced by dynamical decoupling [26–30]. On a complementary perspective, the high degree of selectivity achieved by dynamical decoupling also provides a valuable tool to infer noise characteristics. This fact has opened up a new research streamline named “quantum sensing” [31]. Recently dynamical decoupling of pure dephasing due to quadratic coupling to Gaussian distributed  $1/f^\alpha$  noise has been used as a tool for noise spectroscopy [32]. In this manuscript we will illustrate some sensing properties of two, well-known quantum control protocols, the periodic (PDD) [11,12] and the Carr Purcell (CP) [33] dynamical decoupling (DD). We will discuss critically their capabilities to infer the characteristic of  $1/f$  noise acting on a two-qubit gate. The advantage of applying these procedures to a two-qubit gate are manifold [34]. First of

all, the operating frequency of a two-qubit gate is one-to-two orders of magnitude lower than the Larmor frequency of the individual qubits. This makes the gate more sensitive to low-frequency fluctuations. We will show that this potentially detrimental fact actually turns out to be convenient from the viewpoint of noise sensing. In this article we will focus on this issue. Other potentialities of quantum sensing with a multiqubit gate are the possibility to detect noise correlations [35] or the identification of local effects due to microscopic degrees of freedom more strongly coupled to one of the quantum nodes of a complex network.

## 2. Two Qubit Entangling Gate and Pulsed Quantum Control

Dynamical local control applied to a quantum node of a noisy complex network is generally modelled as

$$\tilde{\mathcal{H}}(t) = \mathcal{H}_0 + \delta\mathcal{H}(t) + \mathcal{V}(t). \quad (1)$$

The noisy quantum node is in our case a two-qubit gate subject to local classical noise

$$\mathcal{H}_0 + \delta\mathcal{H}(t) = -\frac{\Omega}{2}\sigma_{1z} \otimes \mathbb{I}_2 - \frac{\Omega}{2}\mathbb{I}_1 \otimes \sigma_{2z} + \frac{\omega_c}{2}\sigma_{1x} \otimes \sigma_{2x} - \frac{1}{2}z_1(t)\sigma_{1z} \otimes \mathbb{I}_2 - \frac{1}{2}\mathbb{I}_1 \otimes z_2(t)\sigma_{2z}, \quad (2)$$

where  $\mathbb{I}_\alpha$  is the identity in qubit- $\alpha$  Hilbert space ( $\alpha = 1, 2$ ), we set  $\hbar = 1$ . The ideal gate generated by  $\mathcal{H}_0$ , realizes the entangling  $\sqrt{i\text{SWAP}}$  operation: the system prepared in the factorized state  $|+\rangle$  ( $\sigma_{\alpha z}|\pm\rangle_\alpha = \mp|\pm\rangle_\alpha$ ), evolves periodically to the fully entangled state  $\pm[|+\rangle - i|-\rangle]/\sqrt{2}$  at times  $t_e(n) = \pi/2\omega_c(1 + 4n)$ ,  $n \in \mathcal{N}$ . In this, fixed (capacitive or inductive) coupling scheme, individual tuning of each qubit effectively switches on/off their interaction [3].

The local, pure dephasing classical noise,  $z_\alpha(t)$ , is a stochastic process whose power spectrum

$$S_\alpha(\omega) = \int_{-\infty}^{\infty} dt \langle z_\alpha(t)z_\alpha(0) \rangle e^{i\omega t} \quad (3)$$

is  $1/f$  for  $f \in [\gamma_{m,\alpha}, \gamma_{M,\alpha}]$ . Noise is simulated as the superposition of random telegraph (RT) processes with switching rates  $\gamma_\alpha$  distributed as  $1/\gamma_\alpha$  in  $[\gamma_{m,\alpha}, \gamma_{M,\alpha}]$  [4,36]. The spectrum reads  $S_\alpha(\omega) \approx \mathcal{A}_\alpha/\omega$ , with  $\mathcal{A}_\alpha = \pi\Sigma_\alpha^2/\ln(\gamma_{m,\alpha}/\gamma_{M,\alpha})$ , for  $\gamma_{m,\alpha} \ll \omega \ll \gamma_{M,\alpha}$ , with a roll-off to  $1/f^2$  behavior at higher frequencies;  $\Sigma_\alpha^2$  is the noise variance. We will also consider the limiting case of coupling to a single RT process.

We consider dynamical decoupling protocols consisting of instantaneous pulses acting locally and simultaneously on each qubit. In Equation (1) it is  $\mathcal{V}(t) = \mathcal{V}_1(t) \otimes \mathbb{I}_2 + \mathbb{I}_1 \otimes \mathcal{V}_2(t)$ , and  $\mathcal{V}_\alpha(t)$  denotes the action of a sequence of local operations on qubit  $\alpha$  applied at times  $t = t_i$ ,  $i \in \{1, m\}$ . The control sequence is designed to reduce the effect of noise acting along  $\sigma_{\alpha z}$  without altering the gate operation. This is obtained by applying an *even number* of simultaneous  $\pi$ -pulses around the  $y$ -axis of the Bloch sphere of each qubit, denoted respectively as  $\pi_y$ . The pulses are applied at times  $t_i = \delta_i t_e$ , where  $0 \leq \delta_i \leq 1$  with  $i = 1, \dots, m$ . For the PDD sequence  $\delta_i = i/m$ , with the last pulse applied at time  $t_e$ , the pulse interval being  $\Delta t = t_e/m$ . For the CP sequences it is  $\delta_i = (i - 1/2)/m$ .

## 3. Gate Error and Quantum Sensing

Dynamical decoupling aims to maximize the fidelity with respect to the target state  $|\psi_e\rangle$ ,  $\mathcal{F}$ , or equivalently to minimize the error  $\varepsilon$  defined as

$$\mathcal{F} = \langle \psi_e | \rho(t_e^{(n)}) | \psi_e \rangle \quad \varepsilon = 1 - \mathcal{F}. \quad (4)$$

Here  $\rho(t)$  is the two-qubit density matrix and

$$\langle \psi_e | \rho(t_e^{(n)}) | \psi_e \rangle = \int \mathcal{D}[\mathbf{z}(t)] P[\mathbf{z}(t)] \langle \psi_e | \rho(t|\mathbf{z}(t)) | \psi_e \rangle, \quad (5)$$

with  $\mathbf{z}(t) = \{z_1(t), z_2(t)\}$ . We evaluate the path integral by exact numerical solution of the stochastic Schrödinger equation of the coupled-qubits under the action of the considered DD sequences. The number of noise realizations over which the average is performed is  $\geq 10^4$ . Under this condition, the numeric simulation can be considered a reliable method for calculating the gate error.

In the quantum sensing perspective, we aim to grasp informations on the noise spectrum by using the gate as a detector. In this article we focus on pointing out sensitivity to the amplitude of the noise, i.e., its variance, and to the high-frequency cut-off  $\gamma_{M,\alpha}$  the  $1/f$  spectrum. For the sake of simplicity, we suppose identical noise on both qubits,  $S_\alpha(\omega) \equiv S(\omega), \gamma_{m,\alpha} = \gamma_m, \gamma_{M,\alpha} = \gamma_M$ .

### 3.1. Sensitivity to High-Frequency Spectral Components

In order to verify the sensing properties of PDD and CP to components of  $1/f$  noise at high frequencies, we numerically evaluate the gate error at the entangling time  $t_e$ , for a spectrum with fixed variance  $\Sigma^2$ ,  $\gamma_m$ , and varying  $\gamma_M$ . We remark that this implies changing the  $1/f$  noise amplitude,  $\mathcal{A}_\alpha = \pi \Sigma_\alpha^2 / \ln(\gamma_{m,\alpha} / \gamma_{M,\alpha})$ . Results shown in left panel of Figure 1 show that the gate error under PDD is weakly affected by high frequencies in the spectrum until  $\gamma_M < 1/t_e$ . On the contrary, CP DD is more effective in reducing errors and at the same time is more sensitive to changes of  $\gamma_M$ , see left panel of Figure 2. The result for PDD is easily understood considering the propagator for a sequence of two pulses of duration  $\Delta t$  in the presence of quasistatic noise due to a single RT signal with  $\gamma \ll 1/\Delta t$ , and its first order expansion

$$\begin{aligned} U(t_{i+1}, t_{i-1} | \mathbf{x}(t)) &= \mathcal{S} \hat{T} e^{-i \int_{t_i}^{t_{i+1}} \mathcal{H}(t') dt'} \mathcal{S} \hat{T} e^{-i \int_{t_{i-1}}^{t_i} \mathcal{H}(t') dt'} \simeq \\ &\simeq \mathcal{S} \left( \mathbb{I} - i \mathcal{H}(t_i) \Delta t \right) \mathcal{S} \left( \mathbb{I} - i \mathcal{H}(t_{i-1}) \Delta t \right) \simeq \mathbb{I} - i \bar{\mathcal{H}} 2 \Delta t \simeq e^{-i \bar{\mathcal{H}} 2 \Delta t} \end{aligned} \quad (6)$$

where  $\bar{\mathcal{H}} = (\mathcal{S} \mathcal{H} \mathcal{S} + \mathcal{H})/2 = (\omega_c/2) \sigma_{1x} \otimes \sigma_{2x}$  is the entangling term in the Hamiltonian. Equation (6) shows that the lowest order effect of quasistatic noise is cancelled already by a pair of pulses, the so called echo-sequence. As a consequence, PDD sequence with an even number of pulses is able to reduce noise effects at  $t_e = 2n\Delta t$  also in the presence of high-frequency components in the spectrum provided that  $\gamma_M < 1/t_e$ , Figure 1 (right panel). A fast RT fluctuator instead induces a very small error which is unmodified by the decoupling procedure, see the almost flat curve in Figure 1 (right panel). In Figure 2 we repeat the same analysis for CP DD. We observe that CP exhibits larger sensitivity to the  $1/f$  upper cut-off: the gate error can be described by a quasi static approximation up to  $\gamma_M = 10^7 \text{ s}^{-1}$ , that is as long as  $\gamma_M \ll 1/t_e$ . The CP procedure is therefore more suitable to perform sensing of the presence of components of  $1/f$  noise at high-frequencies like inferring its high-frequency cut-off.

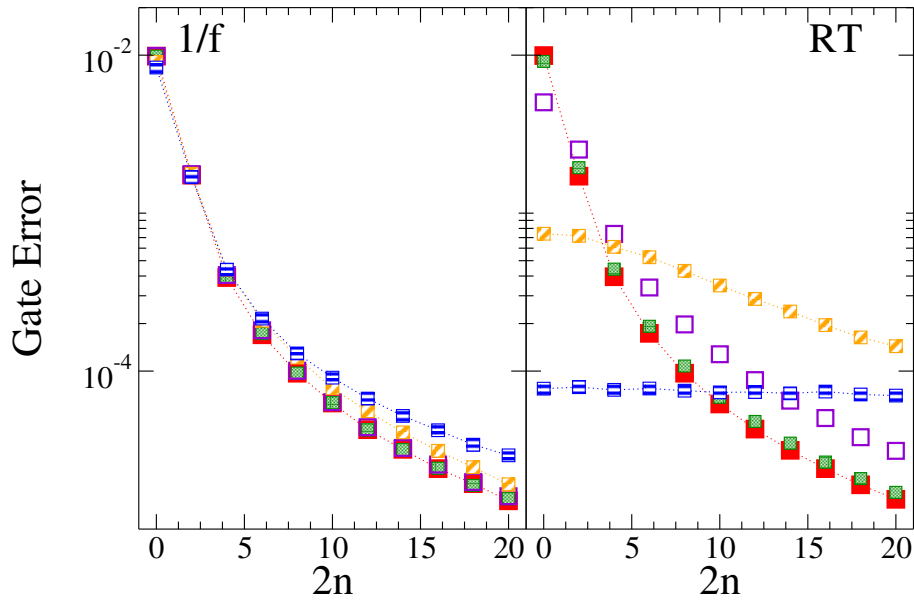


**Figure 1.** Gate error at time  $t_e$  under PDD as function of the number of applied pulses,  $n$ . In each panel  $\omega_c = 5 \cdot 10^9$  rad/s, the standard deviation is  $\Sigma = 10^9 / \sqrt{2}$  rad/s. Left panel: Error for  $1/f$  noise with low frequency cut-off fixed at  $\gamma_m = 1$  s $^{-1}$ . Symbols correspond to different high-frequency cut-off:  $\gamma_M = 1$  s $^{-1}$  (filled red),  $\gamma_M = 10^9$  s $^{-1}$  (shaded green),  $\gamma_M = 10^{10}$  s $^{-1}$  (open violet),  $\gamma_M = 10^{11}$  s $^{-1}$  (oblique orange),  $\gamma_M = 10^{12}$  s $^{-1}$  (horizontal blue). Right panel: Error for RT noise, symbols correspond to different switching rates:  $\gamma = 1$  s $^{-1}$  (filled red),  $\gamma = 10^9$  s $^{-1}$  (shaded green),  $\gamma = 10^{10}$  s $^{-1}$  (open violet),  $\gamma = 10^{11}$  s $^{-1}$  (oblique orange),  $\gamma = 10^{12}$  s $^{-1}$  (horizontal blue). Simulations with  $10^4$  samples.

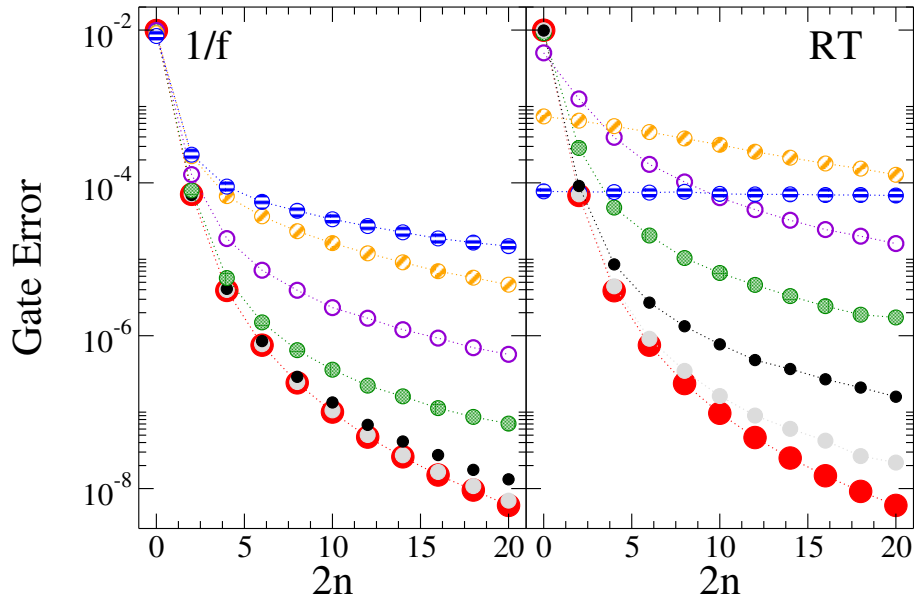


**Figure 2.** Gate error at time  $t_2$  under CP as function of the number of applied pulses,  $n$ . In each panel  $\omega_c = 5 \cdot 10^9$  rad/s, the standard deviation is  $\Sigma = 10^9 / \sqrt{2}$  rad/s. Left panel: Error for  $1/f$  noise with low frequency cut-off fixed at  $\gamma_m = 1$  s $^{-1}$ . Symbols correspond to different high-frequency cut-off:  $\gamma_M = 1$  s $^{-1}$  (filled red),  $\gamma_M = 10^7$  s $^{-1}$  (filled grey),  $\gamma_M = 10^8$  s $^{-1}$  (filled black),  $\gamma_M = 10^9$  s $^{-1}$  (shaded green),  $\gamma_M = 10^{10}$  s $^{-1}$  (open violet),  $\gamma_M = 10^{11}$  s $^{-1}$  (oblique orange),  $\gamma_M = 10^{12}$  s $^{-1}$  (horizontal blue). Right panel: Error for RT noise, symbols correspond to different switching rates:  $\gamma = 1$  rad/s (filled red),  $\gamma = 10^7$  s $^{-1}$  (filled grey),  $\gamma = 10^8$  s $^{-1}$  (filled black),  $\gamma = 10^9$  s $^{-1}$  (shaded green),  $\gamma = 10^{10}$  s $^{-1}$  (open violet),  $\gamma = 10^{11}$  s $^{-1}$  (oblique orange),  $\gamma = 10^{12}$  s $^{-1}$  (horizontal blue). Simulations with  $10^4$  samples.

### 3.2. Sensitivity to the Noise Variance

Scaling of the gate error under DD with the noise variance represents a distinctive feature of the dominant order of the fluctuation statistics [34]. This is relevant in the perspective of using the two-qubit gate as noise detector pointing out Gaussian or non-Gaussian noise statistics. In Figures 3 and 4, we study the scaling of the gate error with the noise variance for the considered DD sequences. Left panels refer to the quasistatic regime, in right panels  $1/f$  noise extends to  $\gamma_M = 10^9 \text{ s}^{-1}$  for PDD, to  $\gamma_M = 10^8 \text{ s}^{-1}$  for CP DD. The reference case corresponds to  $\Sigma = 10^9 \text{ rad/s}$  (filled symbols) which scales with  $\Sigma^2$  (dotted line). In each figure symbols are the results of the exact numerical solution of the stochastic Schrödinger equation and colored dashed lines are the scaling with  $\Sigma^2$  obtained from the reference curve. The gate error under PDD reveals second order statistics effect, both for quasistatic noise and for higher frequency noise components. This is signalled by the  $\Sigma^2$  scaling of all curves. This picture does not hold for the gate error under the CP sequence. In fact, even for quasistatic noise we observe  $\Sigma^2$  scaling only up a certain value of  $\Sigma$ , Figure 4 (left panel). This behavior suggests that higher order noise cumulants contribute to the gate error with increasing noise strength. These contributions maintain their relevance also when the noise extends to higher frequencies, at least up to  $\gamma_M = 10^8 \text{ s}^{-1}$ , Figure 4 (right panel).

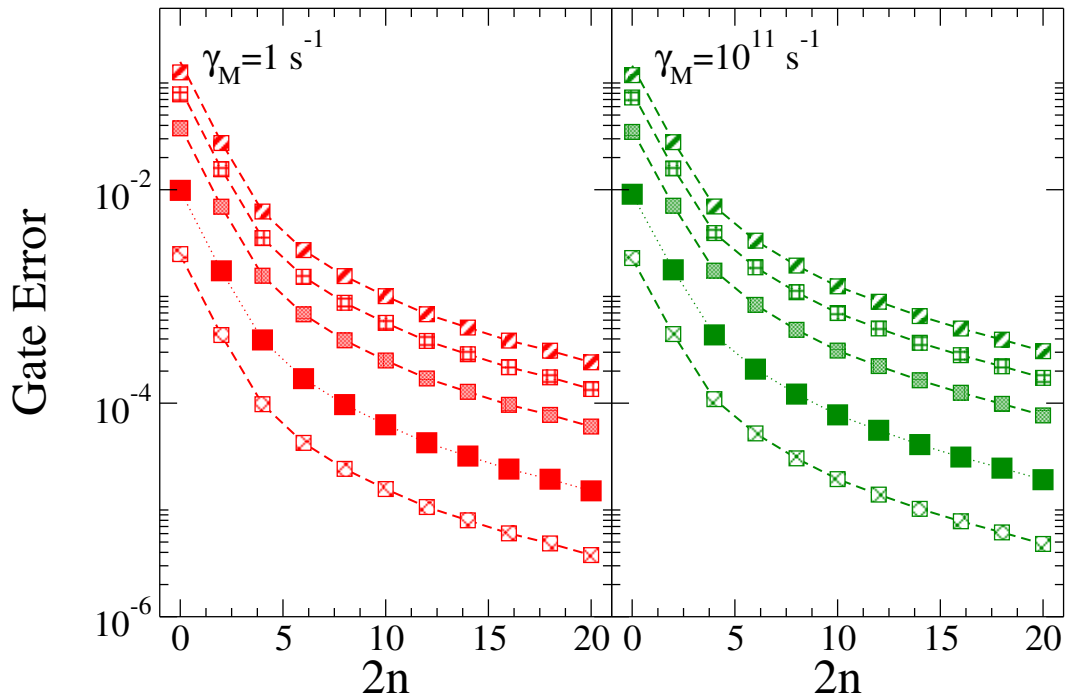


**Figure 3.** Gate error under PDD at time  $t_e$  as function of  $n$ ,  $\omega_c = 5 \cdot 10^9 \text{ rad/s}$ . Left panel: quasi static noise,  $\gamma_m = \gamma_M = 1 \text{ s}^{-1}$ . Right panel:  $1/f$  noise with  $\gamma_m = 1 \text{ s}^{-1}$  and  $\gamma_M = 10^9 \text{ s}^{-1}$ . Curves have different standard deviation:  $\Sigma = 0.5 \cdot 10^9 / \sqrt{2} \text{ rad/s}$  (oblique crossed lines),  $\Sigma = 10^9 / \sqrt{2} \text{ rad/s}$  (filled),  $\Sigma = 2 \cdot 10^9 / \sqrt{2} \text{ rad/s}$  (shaded),  $\Sigma = 3 \cdot 10^9 / \sqrt{2} \text{ rad/s}$  (crossed lines),  $\Sigma = 4 \cdot 10^9 / \sqrt{2} \text{ rad/s}$  (oblique lines). In each panel the dotted line interpolating the gate error for the reference value  $\Sigma = 10^9 / \sqrt{2} \text{ rad/s}$  is a guideline for the eye; dashed lines are obtained by scaling with  $\Sigma^2$  the error corresponding to the reference variance. Simulations with  $10^4$  samples.

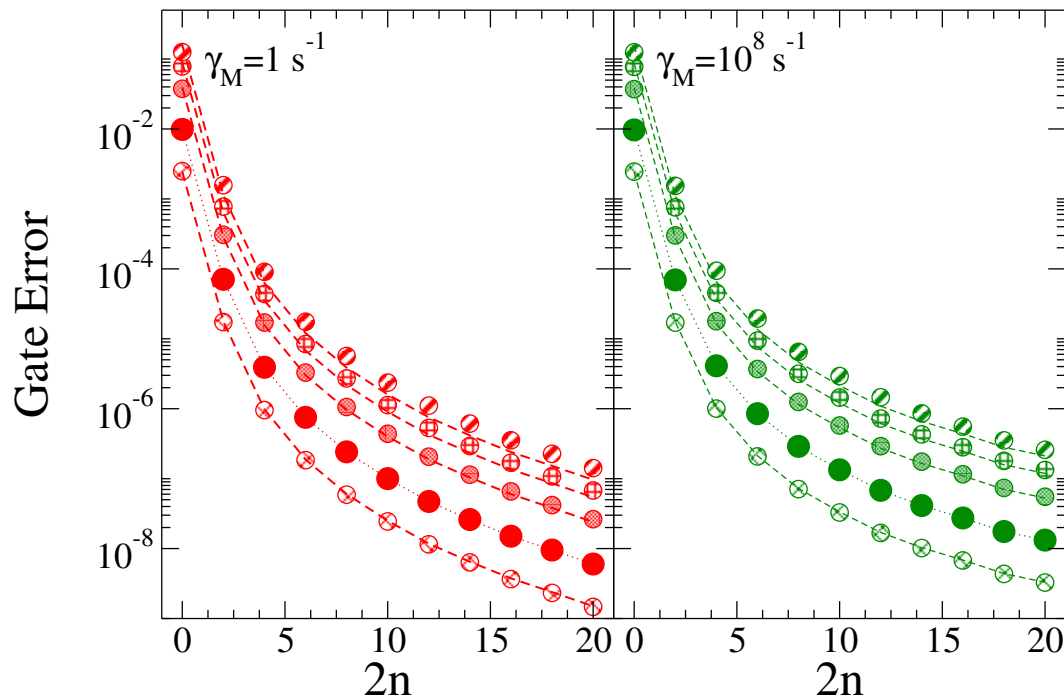


**Figure 4.** Gate error under CP at time  $t_e$  as function of  $n$ . In each panel  $\omega_c = 5 \cdot 10^9$  rad/s, the gate time is  $t_e$ . Left panel: quasi static noise,  $\gamma_m = \gamma_M = 1 \text{ s}^{-1}$ . Right panel:  $1/f$  noise with  $\gamma_m = 1 \text{ s}^{-1}$  and  $\gamma_M = 10^8 \text{ s}^{-1}$ . Curves have different standard deviation:  $\Sigma = 0.5 \cdot 10^9 / \sqrt{2}$  rad/s (oblique crossed lines),  $\Sigma = 10^9$  rad/s (filled),  $\Sigma = 2/\sqrt{2} \cdot 10^9$  rad/s (shaded),  $\Sigma = 3/\sqrt{2} \cdot 10^9$  rad/s (crossed lines),  $\Sigma = 4/\sqrt{2} \cdot 10^9$  rad/s (oblique lines). In each panel the dotted line interpolating the gate error for the reference value  $\Sigma = 10^9 / \sqrt{2}$  rad/s is a guideline for the eye; dashed lines are obtained by scaling with  $\Sigma^2$  the error corresponding to the reference variance. Simulations with  $10^4$  samples.

#### 4. Discussion

Results presented in this article point out the potentialities of DD protocols implemented in superconducting qubits to infer non trivial properties of non-Markovian noise with  $1/f$  spectrum. In particular, CP DD turns out to be a convenient sensing tool for the high-frequency cut-off of the spectrum. Moreover it is suitable to point out the nature, Gaussian or non Gaussian, of the noise statistics entering the gate error. Second order statistics can instead be inferred by the scaling of the gate error under PDD. Provided noise with same statistical properties act of the two qubits forming the gate, the error scaling under PDD might provide an independent check of the noise variance entering single qubit decoherence factors [37]. Based on the present analysis, we expect that dynamical control could be conveniently used to extract correlations between noise sources acting on different units of a few nodes quantum network.

**Acknowledgments:** Authors acknowledge funding by the INFN, Catania Unit (DYNSMAT).

**Conflicts of Interest:** The authors declare no conflict of interest.

#### References

1. Acín, A.; Bloch, I.; Buhrman, H.; Calarco, T.; Eichler, C.; Eisert, J.; Esteve, D.; Gisin, N.; Glaser, S.J.; Jelezko, F.; et al. The quantum technologies roadmap: a European community view. *New J. Phys.* **2018**, *20*, 080201, doi:10.1088/1367-2630/aad1ea.
2. Buluta, I.; Ashab, S.; Nori, F. Natural and artificial atoms for quantum computation. *Rep. Prog. Phys.* **2011**, *74*, 104401, doi:10.1088/0034-4885/74/10/104401.
3. Clarke, J.; Wilhelm, F.K. Superconducting quantum bits. *Nature* **2008**, *453*, 1031–1042, doi:10.1038/nature07128.

4. Paladino, E.; Galperin, Y.M.; Falci, G.; Altshuler, B.L.  $1/f$  noise: Implications for solid-state quantum information. *Rev. Mod. Phys.* **2014**, *86*, 361, doi:10.1103/RevModPhys.86.361.
5. Paladino, E.; Sassetti, M.; Falci, G.; Weiss, U. Characterization of coherent impurity effects in solid-state qubits. *Phys. Rev. B* **2008**, *77*, 041303, doi:10.1103/PhysRevB.77.041303.
6. Devoret, M.H.; Schoelkopf, R.J. Superconducting circuits for quantum information: An outlook. *Science* **2013**, *339*, 1169–1174, doi:10.1126/science.1231930.
7. Paladino, E.; Mastellone, A.; D'Arrigo, A.; Falci, G. Optimal tuning of solid-state quantum gates: A universal two-qubit gate. *Phys. Rev. B* **2010**, *81*, 052502, doi:10.1103/PhysRevB.81.052502.
8. Chiarello, F.; Paladino, E.; Castellano, M.G.; Cosmelli, C.; D'Arrigo, A.; Torrioli, G.; Falci, G. Superconducting qubit manipulated by fast pulses: Experimental observation of distinct decoherence regimes. *New J. Phys.* **2012**, *14*, 023031, doi:10.1088/1367-2630/14/2/023031.
9. Knill, E. Quantum computing with realistically noisy devices. *Nature* **2005**, *434*, 39, doi:10.1038/nature03350.
10. Paladino, E.; D'Arrigo, A.; Mastellone, A.; Falci, G. Decoherence times of universal two-qubit gates in the presence of broad-band noise. *New J. Phys.* **2011**, *13*, 093037, doi:10.1088/1367-2630/13/9/093037.
11. Viola, L.; Knill, E.; Lloyd, S. Dynamical Decoupling of Open Quantum Systems. *Phys. Rev. Lett.* **1999**, *82*, 2417, doi:10.1103/PhysRevLett.82.2417.
12. Viola, L.; Lloyd, S. Dynamical suppression of decoherence in two-state quantum systems *Phys. Rev. A* **1998**, *58*, 2733, doi:10.1103/PhysRevA.58.2733.
13. Gutmann, H.; Wilhelm, F.K.; Kaminsky, W.M.; Lloyd, S. Compensation of decoherence from telegraph noise by means of an open-loop quantum-control technique. *Phys. Rev. A* **2005**, *71*, 020302, doi:10.1103/PhysRevA.71.020302.
14. Bergli, J.; Faoro, L. Exact solution for the dynamical decoupling of a qubit with telegraph noise. *Phys. Rev. B* **2007**, *75*, 054515, doi:10.1103/PhysRevB.75.054515.
15. Cywinski, L.; Lutchyn, R.M.; Nave, C.P.; Sarma, S.D. How to enhance dephasing time in superconducting qubits. *Phys. Rev. B* **2008**, *77*, 174509, doi:10.1103/PhysRevB.77.174509.
16. Lutchyn, R.M.; Cywinski, L.; Nave, C.P.; Sarma, S.D. Quantum decoherence of a charge qubit in a spin-fermion model. *Phys. Rev. B* **2008**, *78*, 024508, doi:10.1103/PhysRevB.78.024508.
17. Falci, G.; D'Arrigo, A.; Mastellone, A.; Paladino, E. Dynamical suppression of telegraph and  $1/f$  noise due to quantum bistable fluctuators. *Phys. Rev. A* **2004**, *70*, 040101, doi:10.1103/PhysRevA.70.040101.
18. D'Arrigo, A.; Falci, G.; Mastellone, A.; Paladino, E. Quantum control of discrete noise in Josephson qubits. *Physica E* **2005**, *29*, 297–307, doi:10.1016/j.physe.2005.05.027.
19. Faoro, L.; Viola, L. Dynamical Suppression of  $1/f$  Noise Processes in Qubit Systems. *Phys. Rev. Lett.* **2004**, *92*, 117905, doi:10.1103/PhysRevLett.92.117905.
20. Cheng, B.; Wang, Q.H.; Joynt, R. Transfer matrix solution of a model of qubit decoherence due to telegraph noise. *Phys. Rev. A* **2008**, *78*, 022313, doi:10.1103/PhysRevA.78.022313.
21. Rebentrost, P.; Serban, I.; Schulte-Herbruggen, T.; Wilhelm, F.K. Optimal Control of a Qubit Coupled to a Non-Markovian Environment. *Phys. Rev. Lett.* **2009**, *102*, 090401, doi:10.1103/PhysRevLett.102.090401.
22. D'Arrigo, A.; Franco, R.L.; Benenti, G.; Paladino, E.; Falci, G. Hidden entanglement in the presence of random telegraph dephasing noise. *Phys. Scr.* **2013**, *T153*, 014014, doi:10.1088/0031-8949/2013/T153/014014.
23. Bellomo, B.; Compagno, G.; D'Arrigo, A.; Falci, G.; Franco, R.L.; Paladino, E. Entanglement degradation in the solid state: Interplay of adiabatic and quantum noise. *Phys. Rev. A* **2010**, *81*, 062309, doi:10.1103/PhysRevA.81.062309.
24. Franco, R.L.; D'Arrigo, A.; Falci, G.; Compagno, G.; Paladino, E. Preserving entanglement and nonlocality in solid-state qubits by dynamical decoupling. *Phys. Rev. B* **2014**, *90*, 054304, doi:10.1103/PhysRevB.90.054304.
25. D'Arrigo, A.; Falci, G.; Paladino, E. Dynamical decoupling of local transverse random telegraph noise in a two-qubit gate. *Phys. Scr.* **2015**, *2015*, 014037, doi:10.1088/0031-8949/2015/T165/014037.
26. Bylander, J.; Gustavsson, S.; Yan, F.; Yoshihara, F.; Harrabi, K.; Fitch, G.; Cory, D.G.; Nakamura, Y.; Tsai, J.S.; Oliver, W.D. Noise spectroscopy through dynamical decoupling with a superconducting flux qubit. *Nat. Phys.* **2011**, *7*, 565–570, doi:10.1038/nphys1994.
27. Yan, F.; Bylander, J.; Gustavsson, S.; Yoshihara, F.; Harrabi, K.; Cory, D.G.; Orlando, T.P.; Nakamura, Y.; Tsai, J.S.; Oliver, W.D. Spectroscopy of low-frequency noise and its temperature dependence in a superconducting qubit. *Phys. Rev. B* **2012**, *85*, 174521, doi:10.1103/PhysRevB.85.174521.



28. Yuge, T.; Sasaki, S.; Hirayama, Y. Measurement of the Noise Spectrum Using a Multiple-Pulse Sequence. *Phys. Rev. Lett.* **2011**, *107*, 170504, doi:10.1103/PhysRevLett.107.170504.
29. Wang, Y.; Rong, X.; Feng, P.; Xu, W.; Chong, B.; Su, J.H.; Gong, J.; Du, J. Preservation of Bipartite Pseudoentanglement in Solids Using Dynamical Decoupling. *Phys. Rev. Lett.* **2011**, *106*, 040501, doi:10.1103/PhysRevLett.106.040501.
30. Roy, S.S.; Mahesh, T.S.; Agarwal, G.S. Storing entanglement of nuclear spins via Uhrig dynamical decoupling. *Phys. Rev. A* **2011**, *83*, 062326, doi:10.1103/PhysRevA.83.062326.
31. Kurizki, G.; Alvarez, G.A.; Zwick, A. Quantum Sensing of Noisy and Complex Systems under Dynamical Control. *Technologies* **2017**, *5*, 1, doi:10.3390/technologies5010001.
32. Cywinski, L. Dynamical-decoupling noise spectroscopy at an optimal working point of a qubit. *Phys. Rev. A* **2014**, *90*, 042307, doi:10.1103/PhysRevA.90.042307.
33. Carr, H.Y.; Purcell, E.M. Effects of Diffusion on Free Precession in Nuclear Magnetic Resonance Experiments. *Phys. Rev.* **1954**, *94*, 630, doi:10.1103/PhysRev.94.630.
34. D'Arrigo, A.; Falci, G.; Paladino, E. High-fidelity two-qubit gates via dynamical decoupling of local  $1/f$  noise at the optimal point. *Phys. Rev. A* **2016**, *94*, 022303, doi:10.1103/PhysRevA.94.022303.
35. D'Arrigo, A.; Mastellone, A.; Paladino, E.; Falci, G. Effects of low-frequency noise cross-correlations in coupled superconducting qubits. *New J. Phys.* **2008**, *10*, 115006, doi:10.1088/1367-2630/10/11/115006.
36. Weissman, M.B.  $1/f$  noise and other slow, nonexponential kinetics in condensed matter. *Rev. Mod. Phys.* **1988**, *60*, 537, doi:10.1103/RevModPhys.60.537.
37. Falci, G.; D'Arrigo, A.; Mastellone, A.; Paladino, E. Initial Decoherence in Solid State Qubits. *Phys. Rev. Lett.* **2005**, *94*, 167002, doi:10.1103/PhysRevLett.94.167002.



© 2019 by the authors. Licensee MDPI, Basel, Switzerland. This article is an open access article distributed under the terms and conditions of the Creative Commons Attribution (CC BY) license (<http://creativecommons.org/licenses/by/4.0/>).